JOURNAL OF GEOPHYSICAL RESEARCH, VOL. 102, NO. B8, PAGES 17,771–17,784, AUGUST 10, 1997

Dynamic simulations of slip on a smooth fault in an elastic solid

Yehuda Ben-Zion
Department of Earth Sciences, University of Southern California, Los Angeles

James R. Rice
Department of Earth and Planetary Sciences and Division of Engineering and Applied Sciences
Harvard University, Cambridge, Massachusetts

Abstract. We report on numerical simulations of slip evolution along a two dimensional (slip varies only with depth) vertical strike-slip fault in an elastic half-space, using a framework incorporating full inertial elastodynamics. The model is a follow-up on earlier quasi-static and quasi-dynamic simulations of deformations along smooth fault systems in elastic continua. The fault is driven below a crustal depth of 24 km by a constant plate velocity of 35 mm/yr. Deformation at each fault location in the crustal zone is the sum of slip rate contributions from rate- and state-dependent friction and power law creep, where both processes have temperature-dependent (and hence depth-varying) coefficients and both take place locally under the same stress. The simulations employ two versions of rate- and state-dependent friction: a "slip" law, which requires nonzero velocity for state evolution, and an "ageing/slowness" law, which incorporates state evolution and restrengthening in stationary contact. The assumed constitutive laws and distribution of frictional parameters are compatible with laboratory experiments. The elastodynamic calculations are based on spectral representations of variables and a new algorithm providing a unified computational framework for calculations of long deformational histories containing short periods of rapid instabilities. The simulations show dynamic rupture propagation and wave phenomena not accounted for in the previous quasi-static and quasi-dynamic works. However, the results are qualitatively similar to those obtained by corresponding quasi-static and quasi-dynamic calculations. Slip histories along a smooth fault, simulated here with full elastodynamics for various constitutive laws and model parameters, consist mostly of quasi-periodic large events. This finding indicates that inertial dynamics does not provide a generic mechanism for generating spatio-temporal complexities of slip. On the other hand, calculations done for cases representing, approximately, strongly disordered systems do show rich slip histories with a range of event sizes. This result is compatible with our previous conclusions that the origin of observed broad distributions of earthquake sizes is strong fault zone heterogeneities. The fully dynamic calculations illustrate the evolution of nucleation phases of instabilities associated with accelerating and expanding creep. Final slip values of model earthquakes in full elastodynamic calculations are larger than those of corresponding quasi-static and quasi-dynamic events. The dynamic overshoot in simulations with the slip version of friction is larger than in those employing the ageing/slowness law.

Introduction

The origin of spatio-temporal complexities of earthquakes is a subject of ongoing controversy in the seismological and physics communities (for recent discussion, see *Ben-Zion and Rice* [1995a], *Cochard and Madariaga* [1996], *Knopoff* [1996], *Langer et al.* [1996], *Madariaga and Cochard* [1996], and *Rice and Ben-Zion* [1996]). While various studies suggest that seismic complexities are explainable in a way consistent with observation of fault segmentation and other heterogeneities, arguments linking complexities solely to inertial dynamics are also made. *Rice* [1993], *Ben-Zion and Rice* [1993, 1995a], and *Rice and Ben-Zion* [1996] indicated that some of these claims are unjustified, as they are based on strong implicit heterogeneities in the form of inherent model discreteness. In general, many of the earlier studies paid no attention to the nucleation size h^* (see below) of instabilities associated with the assumed constitutive laws. *Rice* [1993], *Ben-Zion and Rice* [1995a], and *Rice and Ben-Zion* [1996] use models with a finite h^* that is small in comparison with seismogenic zone dimensions, but sufficiently larger than cell size h of the numerical discretization so that results are independent of that discretization. In those cases the representative behavior is as follows: Under continuous slow loading a region of accelerating slip that is nucleated on a fault enlarges quasi-statically until reaching a size comparable to h^*. Then a rapid dynamic break out of slip occurs, and the rupture zone grows to a much larger size, typically occupying most or all of the seismogenic thickness. Consequently, in such simulations there are very few or no small events and hence no slip complexity in the form of a broad range of ruptures with dimensions smaller than the seismogenic depth. This view of the nucleation process, and transition from initially quasi-static to dynamic slip, is consistent with results of *Shibazaki*

Paper number 97JB01341.
0148-0227/97/97JB-01341$09.00

and Matsu'ura [1992] and *Ohnaka* [1996] for the slip-weakening constitutive model, and results of *Okubo* [1989] and *Dieterich* [1992] for rate- and state-dependent friction laws.

Distinctly different results, often including small event complexity, are found when the numerical procedures do not simulate a continuum limit, because $h > h^*$ instead of satisfying the requirement $h << h^*$. We have called such models "inherently discrete." The inherently discrete condition $h > h^*$ can occur when the friction law embodies abrupt strength drop with slip or when it has pure velocity-dependent strength (without displacement-dependent features of state evolution), since in those cases $h^* = 0$. Such discreteness can also occur with finite h^* simply because of inadequate grid refinement. *Ben-Zion and Rice* [1995a] give examples of each type and argue that such inherently discrete models, which produce small event complexity, provide an approximate representation of strong local heterogeneities, like fault segments, which can stop rupture within the fault zone.

Some other modeling studies, however, have suggested stronger possible links between dynamics on a uniform fault, or fault segment, and complex slip sequences. The appendix summarizes key results and remaining uncertainties in recent works [*Cochard and Madariaga*, 1996; *Langer et al.*, 1996; *Myers et al.*, 1996] that fall in the above category. The resolution of all the issues raised in the appendix will require various separate works. In the present paper we provide an analysis of a two-dimensional (2-D) dynamic fault model governed by lab-based, depth-variable properties. We have recently developed a code for simulating earthquake cycles along a vertical strike-slip fault in an elastic half-space, using a framework incorporating rate- and state-dependent friction and inertial elastodynamics. The elastodynamic calculations are based on the spectral formulation of *Perrin et al.* [1995] and a new algorithm [*Ben-Zion and Rice*, 1995b; *Zheng et al.*, 1995; *Rice and Ben-Zion*, 1996; G. Zheng et al., manuscript in preparation, 1997 (hereinafter referred to as G. Zheng et al., 1997)] which allows accurate treatment, within a single computational framework, of long slow deformation phases on the order of 100 years, short periods of rapid dynamic instabilities on the order of seconds, and the transitions between those modes. This model has natural boundary, (evolving) initial, loading, and arrest conditions, and it provides a proper framework for simulations over many earthquake cycles that can deliver definitive results on the capacity of inertial dynamics to generate complexity on a smooth fault.

We perform such fully dynamic calculations associated with rate- and state-dependent frictional parameters centered around values measured in the lab. The examined cases incorporate various degrees of heterogeneities in the form of pore pressure variations with depth and random fluctuation of friction parameters. In all cases other than one exception, which serves as a contrasting example, the condition $h << h^*$ is satisfied, where h^* is nucleation size of slip instability based on weakening distance and other parameters of the rate- and state-dependent friction [*Rice*, 1993]. Thus the basic mathematical structure of the model realizations corresponds (with the one exception) to a smooth fault system in an elastic continuum, although given cases can (and do) incorporate heterogeneities. In all cases h^* is small in comparison with the seismogenic depth. The results show that the degree of simulated slip complexities increases in general with the degree of assumed fault heterogeneities. However, in all cases we find that event populations simulated on a smooth fault system do not have broad frequency-size distributions. The results do not account for the multitude of small- and intermediate-size events observed in nature. Thus the fully dynamic simulations of the present work support our previous conclusions that geometric disorder and/or other strong fault heterogeneities are at the origin of observed earthquake complexities.

We note that there may exist important dynamic contributions to complexities that are not simulated by the present work. In the case of a smooth homogeneous fault, such may be related to rapid weakening of frictional properties at high slip velocities [e.g., *Heaton*, 1990; *Cochard and Madariaga*, 1996; *Tsutsumi and Shimamoto*, 1997], perhaps as in dynamic fluidization of fault gouge [*Melosh*, 1979] and variation of pore pressure at the rupture front due to frictional heating [*Lachenbruch*, 1980]. In the more realistic case where some heterogeneities are present, complexities may result from strong interactions between those and inertial dynamics. Examples include disordering of a dynamic crack front in a three-dimensional (3-D) solid in the presence of small random heterogeneities of fracture energy [*Rice et al.*, 1994; *Perrin and Rice*, 1994; *Ben-Zion and Morrissey*, 1995; *Morrissey and Rice*, 1996] and dynamic variations of normal stress on a fault separating different elastic materials [*Weertman*, 1980; *Andrews and Ben-Zion*, 1997; *Harris and Day*, 1997]. Also, rotation at high rupture velocities of maximum stress away from the continuation of the fault [e.g., *Yoffe*, 1951; *Rice*, 1980] and other dynamic mechanisms of nonplanar faulting [e.g., *Sharon et al.*, 1995] are likely to be associated with complex histories of slip. While our work confirms that inertial dynamics alone does not provide a generic mechanism for sustained generation of slip complexities, the implications for complexity of most of the above dynamic phenomena remain to be fully understood.

Model

Our canonical representation of a smooth fault system in a continuum solid is based on the models of *Tse and Rice* [1986] and *Rice* [1993] for a fault governed by rate- and state-dependent friction. The calculations here incorporate full inertial elastodynamics. We consider a 2-D strike-slip fault in a 3-D elastic half-space (Figure 1). The fault is loaded by a constant plate velocity $V_{pl} = 35$ mm/yr, imposed over the depth section below 24 km. The resulting deformation at the top 24 km of the fault is governed by two processes: a brittle slip controlled by rate- and state-dependent friction [e.g., *Dieterich*, 1979, 1981; *Ruina*, 1983], and creep motion following power law dependency of creep slip-rate on stress [*Rice*, 1994a; *Ben-Zion*, 1996]. Both deformational processes depend on the (same) local stress, and both are functions of spatial distributions of related parameters. In the simulations discussed here, slip δ is constrained to vary only with depth z (and time t). Thus all model quantities are independent of distance along strike x, and the simulations correspond to 2-D cases. Extensions of the generic simulation procedure discussed below to 3-D cases of dynamic rupture, where slip is function of both spatial coordinates x and z, are given by *Geubelle and Rice* [1995] and *Cochard and Rice* [1997]. However, the implementation of the 3-D dynamic formulation for calculations of long slip histories is, in general, too

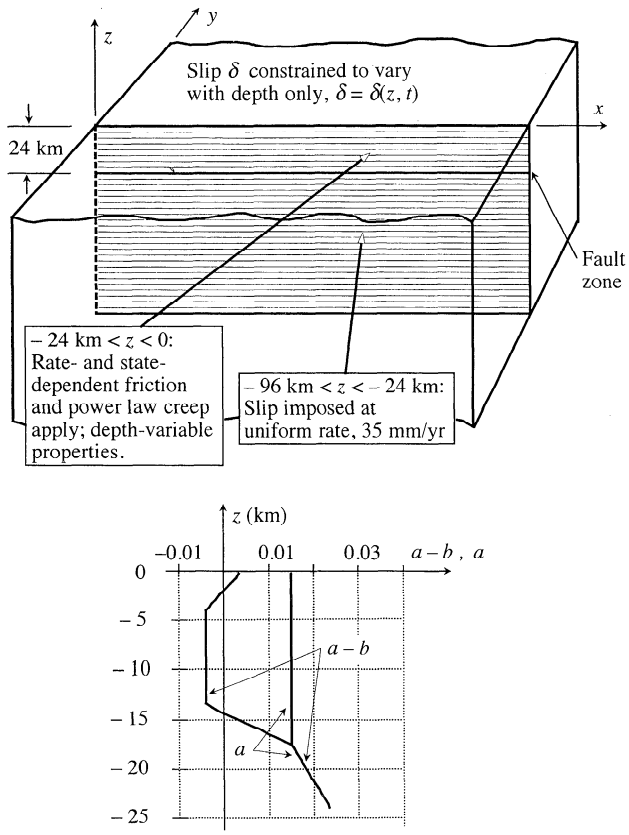

Figure 1. A vertical strike-slip fault in an elastic half-space and assumed reference depth-variation of frictional parameters (adapted from *Rice*, 1993).

computationally demanding, in terms of memory and processor speed, for regular serial computers.

The shear stress on the fault, satisfying continuum elasticity and governed by the above processes, can be written for our 2-D cases as

$$\tau(z, t) = \tau^0(z) + \phi(z, t) - \mu V(z, t) / 2\beta , \qquad (1)$$

where τ^0 is initial stress, ϕ is elastodynamic stress transfer at (z, t) due to previous slip on the fault, V is slip velocity, and μ and β are rigidity and shear wave speed, respectively. The last term in (1), sometimes referred to as radiation damping, gives the instantaneous reduction of stress at a point having slip velocity V. The slip velocity is the sum of two contributions, $V(z, t) = V_{frict}(z, t) + V_{crp}(z, t)$, where V_{frict} is frictional slip rate and V_{crp} is creep velocity. The elastodynamic stress functional ϕ can be written [e.g., *Andrews*, 1985; *Cochard and Madariaga*, 1994; *Perrin et al.*, 1995] as a space-time convolution of a kernel stress transfer function and slip deficit history $\delta(z', t') - V_{pl} t'$ over the information wave cone $|z - z'| < \beta(t - t')$ that is influencing the point (z, t). *Rice and Ben-Zion* [1996] explain the spectral implementation of such convolution in the present modeling context. We calculate the elastodynamic stress transfer ϕ with a novel procedure that allows us to simulate, within a single computational framework, long histories of slow deformation containing short episodes of rapid instabilities. We note that the quasi-dynamic approximation of *Rice* [1993] amounts to replacing ϕ by its long-term static value corresponding to the current slip distribution, so that the actual wave mediation of stress transfers at finite (wave) speeds is neglected. A general discussion of the formulation and initial calculations of fully dynamic ruptures of the type simulated here are given by *Rice and Ben-Zion* [1996] and *Ben-Zion and Rice* [1995b]. A detailed description of the method, and comparison of test cases against analytical and alternative numerical results, are given by *Zheng et al.* [1995] and G. Zheng et al. (1997). Here we summarize the main ingredients, which consist of the following five items:

Spectral representation of the elastodynamic response of a solid. We write slip deficit $\delta(z', t') - V_{pl} t'$ as a Fourier series in z that is truncated at high order and has Fourier coefficients $D_n(t)$. Then the functional $\phi(z, t)$ has a similar series representation with coefficients $F_n(t)$ that can be separated into a final static term given by a factor times $D_n(t)$, and a transient dynamic term given by a convolution integral involving past coefficients $D_n(t')$, $t' < t$.

Use of variable time steps to calculate field values during the deformational evolution of the system. The choice of variable evolutionary time step is governed by requirements for accurate integration of the rate- and state-dependent friction and power law creep constitutive laws, and by recent rates of changes of fields.

Use of a separate computational time domain to calculate the convolution integrals containing the elastodynamic stress transfer ϕ. The calculations of ϕ are done here with equal time steps governed by sampling requirements for accurate evaluation of the convolution on time for each Fourier mode in the slip distribution.

A mapping to obtain field values at times needed for calculations of the elastodynamic convolution integrals, from those calculated at the variable evolutionary time steps. This step can be eliminated if the evolution time steps are chosen as multiples of the elastodynamic time steps.

Truncation of the convolution integrals at appropriate finite ranges. Two important features of our method make the truncations possible. These are the separation of the static term from the dynamic convolution integral as discussed in (1) and the fact that the dynamic convolution integral in our representation has a rapidly decaying kernel. The truncations are done when incremental contributions to the convolution integrals are below a specified value or when the maximum allocated size of the elastodynamic time window has been reached.

Ben-Zion and Rice [1995b], *Zheng et al.* [1995], and G. Zheng et al. (1997) explored various options for calculating the convolution integrals and mapping values from the evolutionary time domain to the elastodynamic one. Here we employ a version involving a constant length in time for the various spectral modes (in contrast to constant number of kernel cycles) and simple linear mapping from the evolutionary time domain to the elastodynamic window (see G. Zheng et al. (1997) for details). In the calculations below, the allocated size of the elastodynamic window is 30 times the period required for an elastic wave to cross the seismogenic zone. This maximum allocated size is rarely reached in the simulations.

We consider two versions of the rate- and state-dependent friction laws of type developed by *Dieterich* [1979, 1981] and *Ruina* [1983]. Following the terminology of *Ruina* [1983], *Beeler et al.* [1994] and *Perrin et al.* [1995], these are a Dieterich-Ruina "ageing" or "slowness" version, in which

strength evolves with both slip and hold time of truly stationary contact, and a Ruina-Dieterich "slip" version, in which friction evolves only with ongoing slip. In both cases the frictional shear strength S is given by

$$S / [\sigma_n - p] = f = f_0 + a \ln(V_{frict} / V_0) + b \ln(V_0 \theta / L) , \quad (2)$$

where σ_n is normal stress, p is pore pressure, f is coefficient of friction, f_0 is nominal friction fixed at a value of 0.5, V_0 is reference velocity set equal to the assumed V_{pl} of 35 mm/yr, a gives the instantaneous frictional response to a step change in sliding velocity V_{frict}, b characterizes the amplitude of evolutionary slip-dependent change of friction, L is characteristic slip distance (sometimes called D_c) over which the evolutionary effect occurs, and θ is state variable. In the case of the ageing or slowness version the state variable satisfies

$$d\theta/dt = 1 - V_{frict} \theta / L , \quad (3a)$$

whereas in the slip version

$$d\theta/dt = - (V_{frict} \theta / L) \ln(V_{frict} \theta / L) . \quad (3b)$$

In both cases, during steady state sliding (constant sliding velocity for slip distance larger than L), $\theta = L / V_{frict}$ and the steady state dependency of the friction coefficient on the sliding velocity is

$$f_{ss} = f_0 + (a - b) \ln(V_{frict} / V_0) . \quad (4)$$

Expression (2) as written contains singularities at very low and very high values of frictional velocity. In the simulations that follow we regularize the equation near $V_{frict} = 0$ by inverting the expression to an exponential form for V_{frict} and then replacing $\exp(f/a)$ by $2 \sinh(f/a)$ [*Rice and Ben-Zion*, 1996]. This regularization assures that as one of f or V_{frict} tends to zero, so does the other. We also impose on the $\ln(V_{frict} / V_0)$ term of (2) an upper limit cutoff at $V_{frict} = 10$ m/s, with the term being independent of V_{frict} at higher speeds (this cutoff avoids numerical overflow in a Newton-Rhapson solution of (1) for V and τ at each time step), and we replace V_{frict} by $|V_{frict}|$ in equations (3a) and (3b) for $d\theta/dt$. Additional explanations on equations (2)-(4) can be found in the works of *Ben-Zion and Rice* [1995a] and *Rice and Ben-Zion* [1996], who used similar expressions.

The creep stress-slip process is governed, as in *Rice* [1994a] and *Ben-Zion* [1996], by a power law dependency of creep slip-rate V_{crp} on stress

$$V_{crp}(z, t) = c(z) \tau(z, t)^3 , \quad (5a)$$

where $c(z)$ is a spatial distribution of creep coefficients given by

$$c(z) = P \exp\{Q (|z| - z_{BD})\} . \quad (5b)$$

This relation represents a rapid increase of $c(z)$ with temperature and hence with depth $|z|$. Here, P and Q are constants discussed further below, and z_{BD} is a nominal brittle-ductile transition depth. The constant P is given by

$$P = V_{pl} / \{[f_0 \sigma_{eff}(z_{BD})]^3\} , \quad (5c)$$

where $\sigma_{eff}(z_{BD})$ is lithostatic overburden minus pore pressure at $|z| = z_{BD}$. This choice makes V_{crp} at z_{BD} equals the plate velocity V_{pl}, if the stress there is $\tau = f_0 \sigma_{eff}(z_{BD})$. The constant Q is chosen as

$$Q = 3.0 \ln(\tau_{ratio}) / (z_{UC} - z_{BD}) . \quad (5d)$$

Relation (5d) enforces the ratio τ_{ratio} between the stress at z_{BD} and that at z_{UC}, if both locations have the same V_{crp}, i.e., if $V_{crp}(z_{BD}) = V_{crp}(z_{UC})$.

In some of the simulations discussed below, the creep process is disabled, and the only operating deformational mechanism is that due to the rate- and state-dependent friction. In the simulations incorporating the creep process we use z_{BD} = 18 km, $\tau_{ratio} = 5$, and z_{UC} = 24 km.

Results

The simulations that follow make use of various distributions of pore pressure p and frictional parameters a and b with depth. Our standard reference case is a situation in which p is hydrostatic and a and b are given by the line fit of *Rice* [1993], reproduced here as part of Figure 1, to the laboratory measurements of *Blanpied et al.* [1991]. These frictional parameters correspond to potentially unstable velocity-weakening regime ($b > a$) in the approximate depth range 4.0 km < $|z|$ < 13.5 km and inherently stable velocity-strengthening regime ($a > b$) in the shallower and deeper sections. Some model realizations of a smooth fault system incorporate heterogeneities in the form of static variations of p between hydrostatic and lithostatic gradients as in *Ben-Zion and Rice* [1995a, Figure 11] and random fluctuations of a and b. The assumed pore pressure heterogeneities represent simple cases of fault structures having over given depth ranges highly elevated p. The assumed random fluctuations of a and b provide crude examples of isolated heterogeneities leading to strong localized variations of stress drops. The simulations do not account for more general cases, in which p varies not only with space but also with time [e.g., *Sleep and Blanpied*, 1992; *Lockner and Byerlee*, 1995; *Miller et al.*, 1996; *Miller*, 1996] and where stress drop variations are not necessarily localized but can be correlated in space [e.g., *Ben-Zion and Rice*, 1995a, Figure 2c].

The model consists of a (partially) seismogenic upper crust layer in the section 0 < $|z|$ < 24 km, where slip is calculated, over a lower crust and upper mantle region in the depth range 24 km < $|z|$ < 96 km, where slip is imposed. During calculations, values of variables in the above system are reflected through the depth $|z|$ = 96 km (and z = 0). This approach assures that the stress component τ_{zx} properly vanishes at z = 0 and also makes it vanish at 96 km depth.

The simulations employ numerical cells of equal size (height) h and were done on a Sparc10 workstation. Because of computational limitations we use N_c = 64 numerical cells for the upper crust layer 0 < $|z|$ < 24 km and a total of $2 \cdot (N_c + 3N_c)$ = 512 cells for the entire model. Thus h in the present work is 3/8 km. The assumed constitutive friction law implies a nucleation size for slip instability [*Rice*, 1993] on the order of $h^* = (2/\pi) L \mu / [(b - a) (\sigma_n - p)]$. When the numerical cell size satisfies $h << h^*$, the mathematical structure of the model corresponds to a smooth continuum fault system, and the results are independent of the cell size used. To satisfy the condition $h << h^*$, with h = 3/8 km and $b - a$ as in the works

of *Blanpied et al.* [1991] and *Rice* [1993], we use values of L much larger than those measured in the lab. Thus the sizes of the simulated nucleation zones are unrealistically large. However, issues related to dynamic complexities and other overall qualitative features of the simulated slip histories are not affected by the specific choice of L, as long as $h << h^* << z_{UC}$ (or z_{BD}). In most calculated examples we keep $h = z_{UC}/64 = h^*/4$. In one case, illustrating the behavior of an inherently discrete fault system with our formulation, we use $h = 4h^*$. In all cases L is chosen as the maximum of 2.5 mm and $\pi h^* [(b - a)(\sigma_n - p)] / 2\mu$, giving a depth-variable L with a lower limit cutoff of 2.5 mm. Thus for hydrostatic pore pressure and normal stress equal to overburden, so that $\sigma_n - p = 180$ MPa at 10 km depth, calculations within the continuum limit ($h = h^*/4$) correspond to $L = 156$ mm at that depth, and the inherently discrete calculations ($h = 4h^*$) correspond to $L = 10$ mm. All cases shown incorporate full elastodynamics.

Figure 2 shows 100 years of slow stable deformation obtained with fully dynamic calculations incorporating the slip version of the rate- and state-dependent friction. The additional creep model process is disabled, p is hydrostatic, and $h = h^*/4$. During the portion of model evolution of Figure 2 the shallow and deep velocity-strengthening regimes have ongoing stable slip, while the brittle velocity-weakening regime is locked. After approximately 6.8 years of additional loading due to the constant plate motion at the downward continuation of the fault ($|z| > 24$ km), a model earthquake is initiated in the brittle seismogenic zone. This is shown in Figure 3a, where we plot 80 s (in contrast to the 100 years of Figure 2) of fast model evolution. The earthquake begins with a nucleation phase of accelerating creep which expands in space. When the size of the nucleation zone is approximately equal to h^*, slip instability occurs and rupture propagates dynamically from the nucleation zone. The rupture propagates first to the free surface and is then reflected to the deeper section, triggering a massive slip event. The dynamic phenomena associated with the model earthquake can be seen better in the expanded Figure 3b, where we show the last 15 s of the same event.

Figures 3a and 3b contain "high-resolution" details of nucleation and dynamic rupture associated with a given model earthquake. We next examine long history containing many earthquake cycles, calculated by the same model realization. Figure 4 gives profiles of slip versus depth with 5 year intervals for about 1000 model years. The "low-resolution" profiles of Figure 4 are extracted from dynamic calculations of high-resolution results including the slip histories of Figures 2 and 3. The results show large stick-slip events in the brittle seismogenic zone (details of the first such event are given in Figures 3a and 3b) and ongoing stable slip in the shallower and deeper sections. The slip profiles of Figure 4 are qualitatively very similar to corresponding quasi-static [*Tse and Rice*, 1986] and quasi-dynamic [*Rice*, 1993; *Ben-Zion and Rice*, 1995a] results. The amplitudes of the unstable slip events generated by our fully dynamic calculations are larger than those in corresponding quasi-static or quasi-dynamic simulations. The unstable slip events of Figure 4 are associated with a large (roughly 100%) dynamic overshoot, and during model earthquakes the brittle seismogenic zone jumps ahead of the deeper stable section by a large amount. The dynamic calculations exhibit also rupture propagation and wave phenomena absent in the quasi-static or quasi-dynamic works. However, the results show as before that earthquake history on a smooth fault contains only large (quasi-periodic in the model realization leading to Figures 2-4) events. Slip complexities such as wide range of event sizes are not simulated by our smooth fault model incorporating inertial elastodynamics.

The results of Figures 2-4 were generated by a 2-D model with the slip version of the rate- and state-dependent friction and without heterogeneities. *Rice* [1994b] and *Rice and Ben-Zion* [1996] found in 3-D quasi-dynamic simulations that the alternative slowness/ageing version of the friction law sometimes leads to complex temporal sequence of large events. This result is of course accentuated when the model incorporates heterogeneities. Below we discuss simulations generated with the alternative version of the friction law. We also consider a few cases of strong frictional heterogeneities in smooth fault systems with $h << h^*$, and we examine the effects of the heterogeneities on the resulting slip histories. One way of adding frictional heterogeneities while keeping the smooth mathematical structure of the model, with some physical relevance, is to incorporate in the model pore pressure heterogeneities.

Figure 5 shows profiles of slip versus depth with 2 year intervals, generated by a 2-D fully dynamic model realization with the slowness/ageing friction, $h = h^*/4$, and heterogeneities in the form of strong variations of p with depth as in Figure 11c of *Ben-Zion and Rice* [1995a]. This assumed pore pressure distribution starts as hydrostatic p in

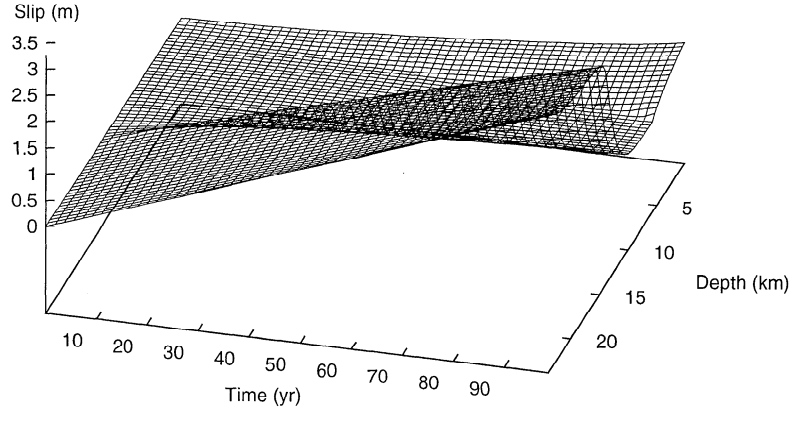

Figure 2. Long stable deformation in dynamic simulation with the "slip" version of the rate- and state-dependent friction. The creep model process is disabled, p is hydrostatic, and $h = h^*/4$.

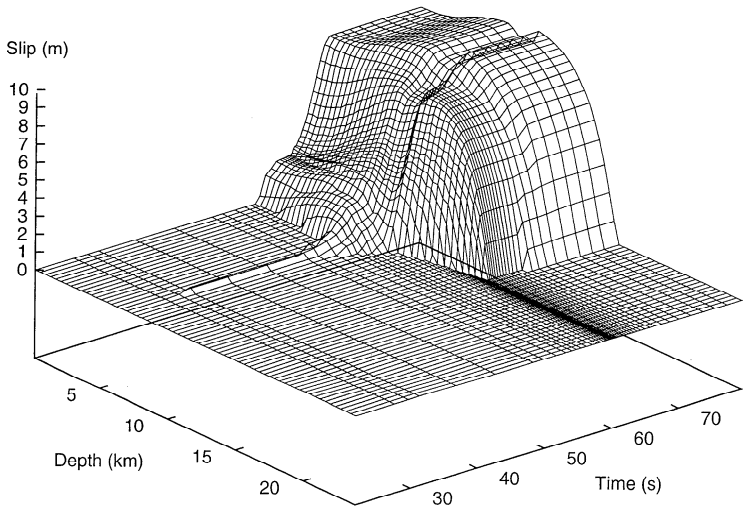

Figure 3a. A dynamic slip event in the model leading to Figure 2. Slip distribution is relative to a given value chosen by the plotting program. The dynamic instability is preceded by a smoothly growing nucleation phase. The apparent abrupt initiation of the nucleation phase and apparent low final slip in the center are plotting artifacts.

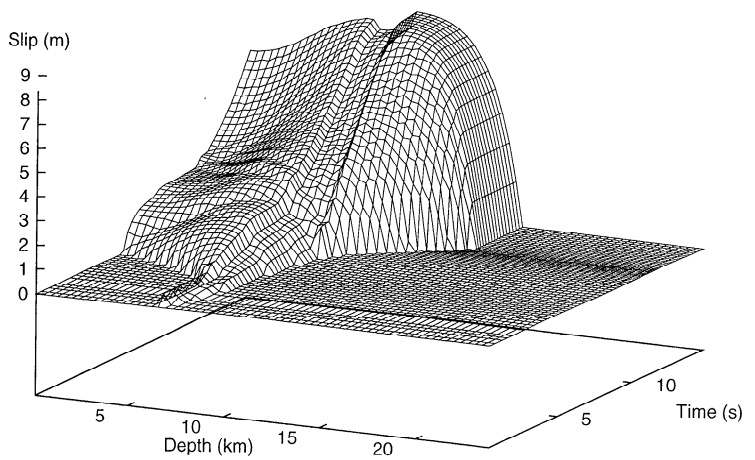

Figure 3b. Last 15 s of the model earthquake. The rupture propagates from the nucleation phase to the free surface and is then reflected downward. Variations of final slip, visible clearly in the shallow zone, are associated with dynamic waves.

the top 6 km. At 6 km depth, p increases abruptly to σ_n – 10 MPa and then continues with lithostatic gradient to 10 km, after which depth p increases with the usual hydrostatic gradient. The simulations incorporate the additional creep process of equations (5a-5d) with z_{BD} = 18 km, τ_{ratio} = 5, and z_{UC} = 24 km. The results show more complexity than Figure 4, and the effect of the abrupt step in p is clearly visible around 6 km depth. However, the simulated slip history still consists only of quasi-periodic large events. The model earthquakes either break the entire seismogenic zone or are arrested near the abrupt step of p. There are no events with dimensions smaller than the length scales characterizing the assumed heterogeneities. The dynamic overshoot in Figure 5 is much smaller than that shown in Figure 4. In general, we find that the slip version of the rate- and state-dependent friction leads to a considerably larger dynamic overshoot than does the slowness/ageing friction, probably because the latter friction incorporates stronger healing mechanism than the former. In addition, model heterogeneities reduce the magnitude of the dynamic overshoot. Figure 6 shows detailed slip distribution associated with one model earthquake of Figure 5. Interestingly, the event has two nucleation phases; the first shallower nucleation phase induces a second deeper one before reaching a size (larger then h^*) that can trigger the instability.

Figure 7 gives slip versus depth profiles with 2 year intervals for another case with the ageing/slowness friction, $h = h^*/4$, and power law creep. Here the distribution of p is given by Figure 11d of *Ben-Zion and Rice* [1995a]. In this case, p has four abrupt steps to σ_n – 10 MPa at depths of 4, 8, 12, and 16 km, and between the steps p follows a hydrostatic gradient. The calculations show more complexity than the previous, less heterogeneous, cases. As may be expected, the slip history of Figure 7 contains smaller events than before. The existence of smaller events is associated with smaller length scales in the assumed distribution of p. While it is clear that the simulated complexity does not embody a Gutenberg-

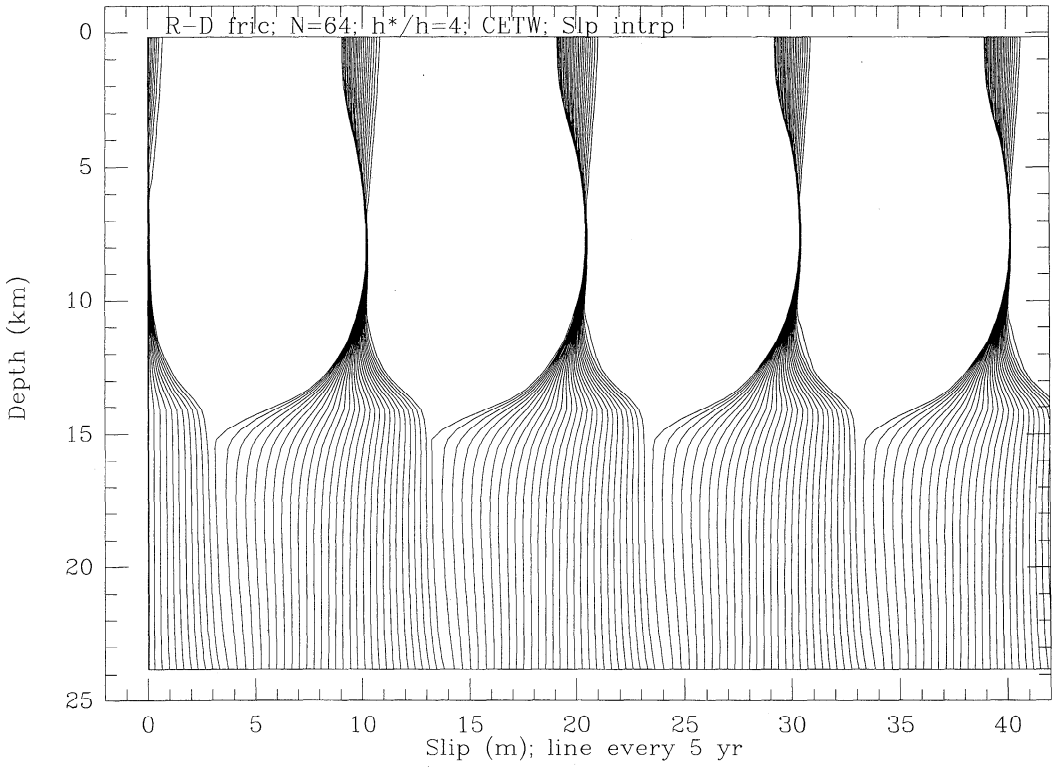

Figure 4. Slip versus depth at 5-year interval in dynamic simulation of long history with the model realization of Figures 2 and 3. The response consists of quasi-periodic large events.

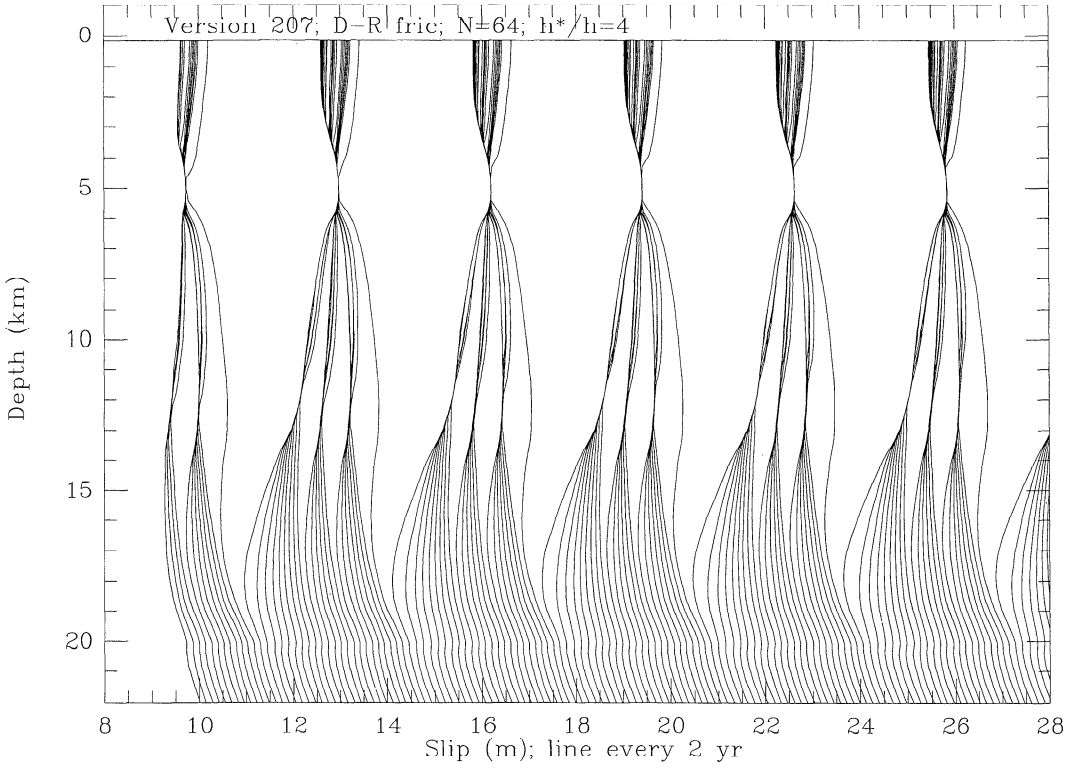

Figure 5. Slip versus depth at 2-year interval in dynamic simulation of long history with the "ageing/slowness" version of the rate- and state-dependent friction. The creep process is active, p has step to 10 MPa offset from σ_n at 6 km and lithostatic gradient to 10 km, and $h = h^*/4$. The response shows slip complexities associated with the strong heterogeneities of p.

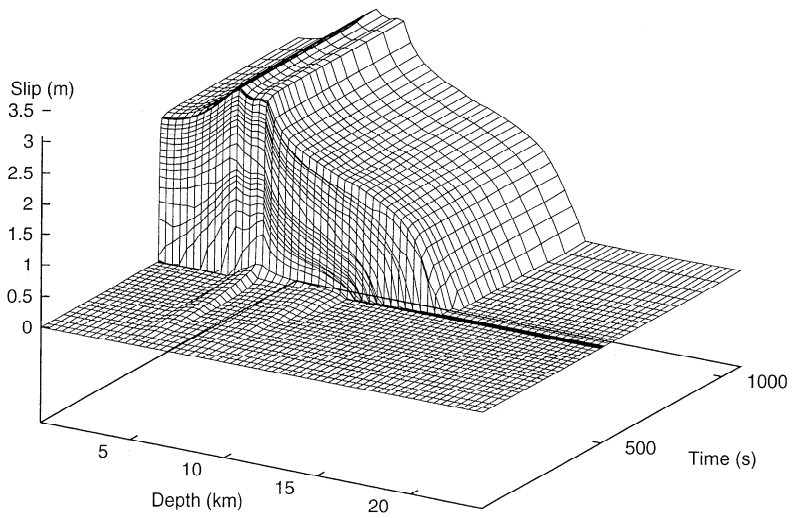

Figure 6. Slip distribution associated with a model earthquake in the simulation leading to Figure 5. The event is preceded by two nucleation phases.

Richter (power law) size distribution for small events, the results suggest that modeling a broad range of length scales of heterogeneities might do so. As with Figure 5, the dynamic overshoot in Figure 7 is much smaller than that present in Figure 4. A detailed example of a model earthquake in this case is shown in Figure 8.

Simulations with other heterogeneities of p [e.g., Figures 11a and 11b, *Ben-Zion and Rice*, 1995a] lead to results that are qualitatively similar to what was shown above. It is interesting to note that some 2-D and 3-D quasi-dynamic simulations, like those of *Rice* [1994b] and *Rice and Ben-Zion* [1996], with the ageing/slowness friction and p given as the maximum of hydrostatic gradient and σ_n – 500 bars [*Ben-Zion and Rice*, 1995a, Figure 11b], produced apparently chaotic sequences of large events. This result has not been seen in our 2-D fully dynamic simulations for a similar case. However, the chaotic 2-D histories mentioned above (J. R. Rice and Y. Ben-Zion, unpublished work, 1996) were found only for much

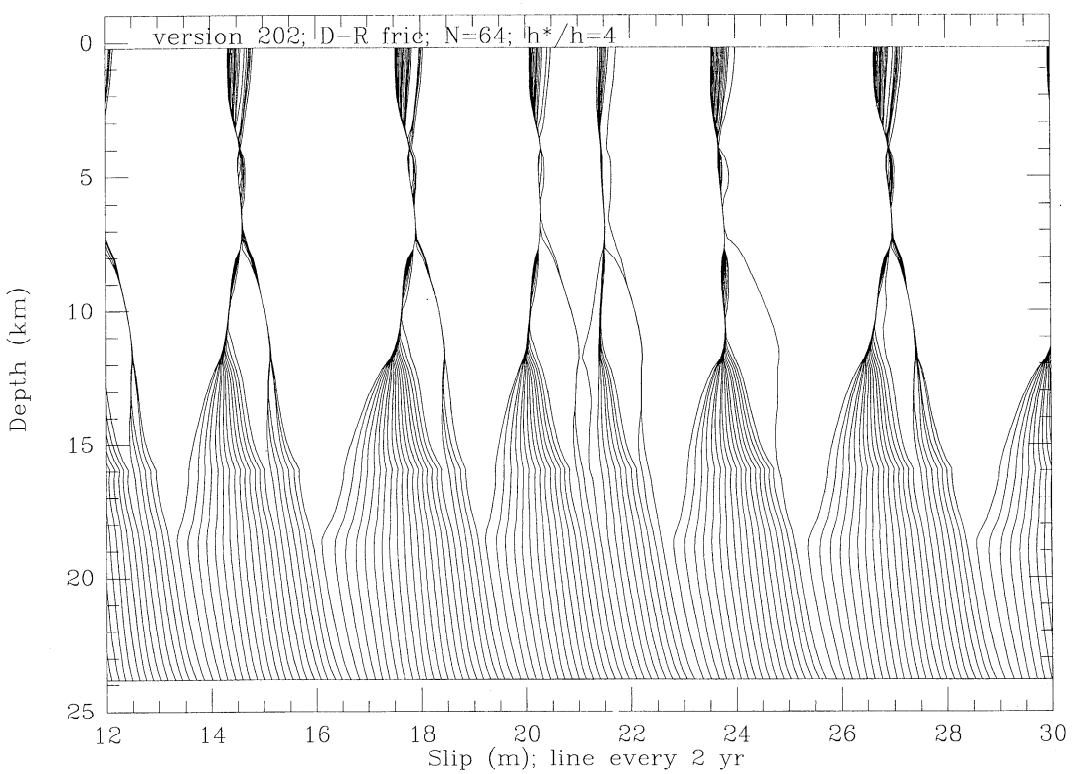

Figure 7. Slip versus depth at 2-year interval in dynamic simulation of long history with the ageing/slowness version of the rate- and state-dependent friction. The creep process is active, p has four steps, each to 10 MPa offset from σ_n, at 4, 8, 12, and 16 km, and $h = h^*/4$. The response shows slip complexities associated with the strong heterogeneities of p.

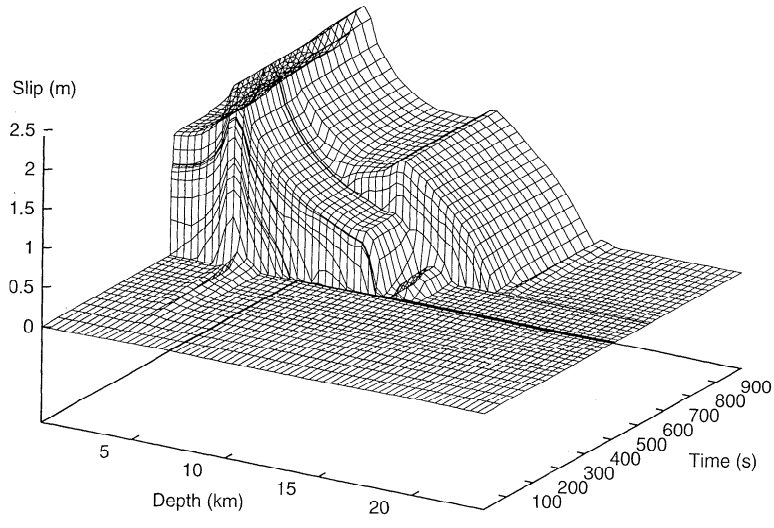

Figure 8. A model earthquake in the simulation leading to Figure 7.

smaller cell size (e.g., $N_c = 512$) and larger ratios of h^*/h (= 8 to 16) than those that we use here and were not seen for $N_c = 128$. The origin of the chaotic 2-D quasi-dynamic histories is not clear at present. However, this is not related to model discreteness (which also leads to complex slip histories), since the large N_c and h^*/h in those cases provide a better approximation to the continuum limit than do the present dynamic simulations. Our use here of $N_c = 64$ is dictated by computational feasibility. However, it is important to repeat in future studies the fully dynamic calculations discussed here with values of N_c and h^*/h comparable to those used in the earlier quasi-dynamic works.

We now examine a case of strong fault zone heterogeneities given in terms of uncorrelated fluctuations of the frictional parameters a and b. We consider a situation in which $a(z)$ and $b(z)$ are increased, with 20% probability, by a factor of 10 from the values used so far. In this case, localized regions, chosen randomly with 20% probability, have stress drops 10 times larger than the lab values of *Blanpied et al.* [1991]. The high stress drop regions provide a simple example of barriers that may stop ruptures and hence increase the complexity of the simulated response. Values of the critical weakening distance L are chosen, as before, based on the assumed distributions of a and b. Thus L is scaled as needed to keep $h^*/h = 4$. This scaling has no lab basis, but it enables us to isolate the calculations from grid size dependency. On the other hand, the random selection with 20% probability of high stress drop barriers introduces into the problem length scales similar to h^*. Thus, while $h < h^*$ is still satisfied, the assumed distribution of heterogeneities leads to rupture zones between the strong barriers of comparable size to that of the nucleation slip size h^*. This suppresses the development of dynamic ruptures, and we distinguish such cases from distributions (for example, the model realizations leading to Figures 2-6) in which the heterogeneities are separated by several times h^*. In the latter situation there is a clear separation of the various length scales, and dynamic ruptures can become well developed (and hence hard to stop) before they encounter heterogeneities. The opposite extreme situation is that of an inherently discrete system $h > h^*$, in which there is no separation of scales, not only between heterogeneities and dynamic ruptures but also between heterogeneities and nucleation phases. We thus regard the above case of uncorrelated random heterogeneities as a borderline between model realizations of a smooth continuum fault and an inherently discrete system. The model leading to Figures 7 and 8, with four abrupt steps of p at depths of 4, 8, 12, and 16 km, comes close to being at a similar border category.

Figure 9 shows profiles of slip versus depth with 2 year intervals for a case with the slowness/ageing friction, a and b as described above, $h = h^*/4$, p = max(hydrostatic, $\sigma_n - 500$ bars), and the additional power law creep process. Figure 10 gives an example of a model earthquake in the same case. The slip distribution of Figure 10 has a small event, separated from and following the main (shallower) earthquake. The small event may be considered as an immediate aftershock to the shallower event, or alternatively, the entire slip distribution may be taken as an example of a multiple-source event. The results of Figure 9 follow the trend seen in the previous cases; the degree of complexity in the simulations increases with the amount of disorder in the assumed properties. The high stress drop barriers are clearly reflected in the response. The dynamic overshoot in Figure 9, with the slowness/ageing friction and strong heterogeneities, is negligible.

The final case we consider is an example of simulation with $h = 4h^*$. As discussed by *Rice* [1993] and *Ben-Zion and Rice* [1993, 1995a], the results in this case are no longer independent of the choice of cell size, and the model is inherently discrete. The situation $h > h^*$ introduces into the problem a length scale of size h, which we have interpreted before as corresponding approximately to a basic unit of fault segmentation or other forms of geometric disorder of faults. In the case $h > h^*$ there is an imposed separation between length scale of local frictional response and length scale governing stress transfer and rupture propagation and arrest. This may be justified [e.g., *Ben-Zion*, 1996] since h^* based on lab values of L, a, and b is on the order of meters, while fault offsets and other structural discontinuities governing macroscopic earthquake ruptures are orders of magnitude larger. However, a rigorous modeling would simulate large-scale structural discontinuities in a framework having $h << h^*$, thus providing a self-consistent treatment of all physical features of the model instead of forcing an approximate separation of scales $h > h^*$ as is done here. Unfortunately, such a treatment is not currently possible with available computational resources.

Figure 11 shows profiles of slip versus depth for an

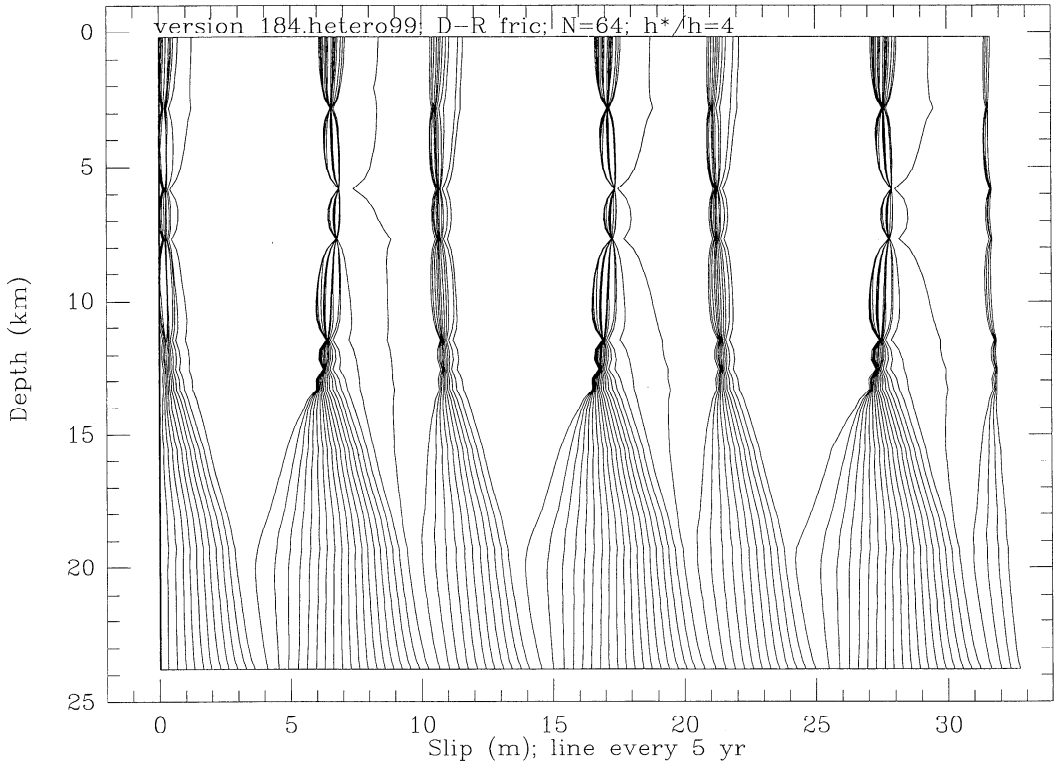

Figure 9. Slip versus depth at 2-year interval in dynamic simulation of long history with the ageing/slowness version of the rate- and state-dependent friction. The frictional parameters include strong uncorrelated random heterogeneities with 20% probability. The creep process is active, p has lithostatic gradient below about 3 km and is offset 50 MPa from σ_n, and $h = h^*/4$. The slip history is more complex than those of the previous, less heterogeneous, cases.

inherently discrete case $h = 4h^*$ with the slip version of friction, hydrostatic p, and the additional creep process disabled. This case is similar to that leading to Figures 2-4, with the important exception that the former results were generated by a smooth fault system, whereas here the model is discrete. Since the results contain smaller-scale features than those of the previous cases, they are plotted with time intervals of 0.3 year. In agreement with the quasi-dynamic simulations of *Rice* [1993] and *Ben-Zion and Rice* [1995a], the fully dynamic response of an inherently discrete model is more complex than the corresponding response (Figure 4) of a smooth continuum fault. The dynamic overshoot in Figure 11 is smaller than that of Figure 4 with no heterogeneities, but larger than the ones in Figures 5, 7, and 9 with the slowness/ageing friction and milder heterogeneities. Figure 12 gives an example of a model earthquake in the inherently discrete case. The event shown has two nucleation phases, as in Figure 6.

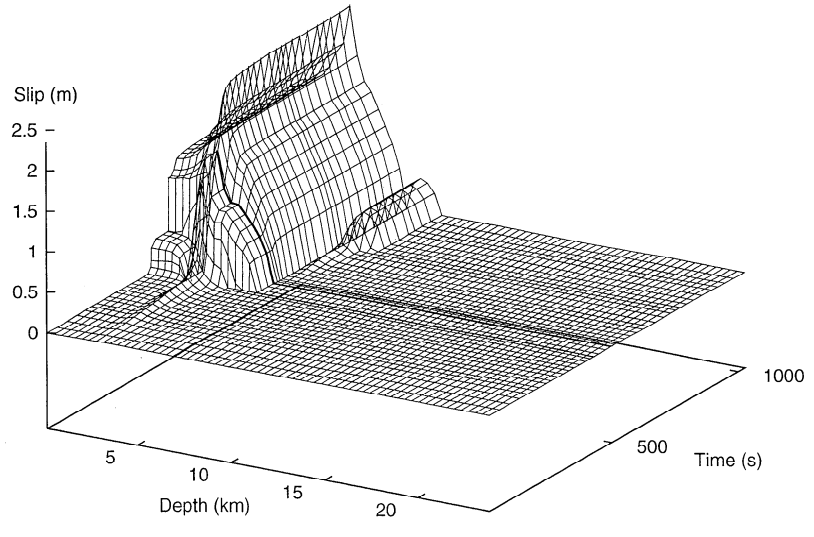

Figure 10. Slip distribution in the simulation leading to Figure 9. The space-time distribution is rough with a small aftershock-like event.

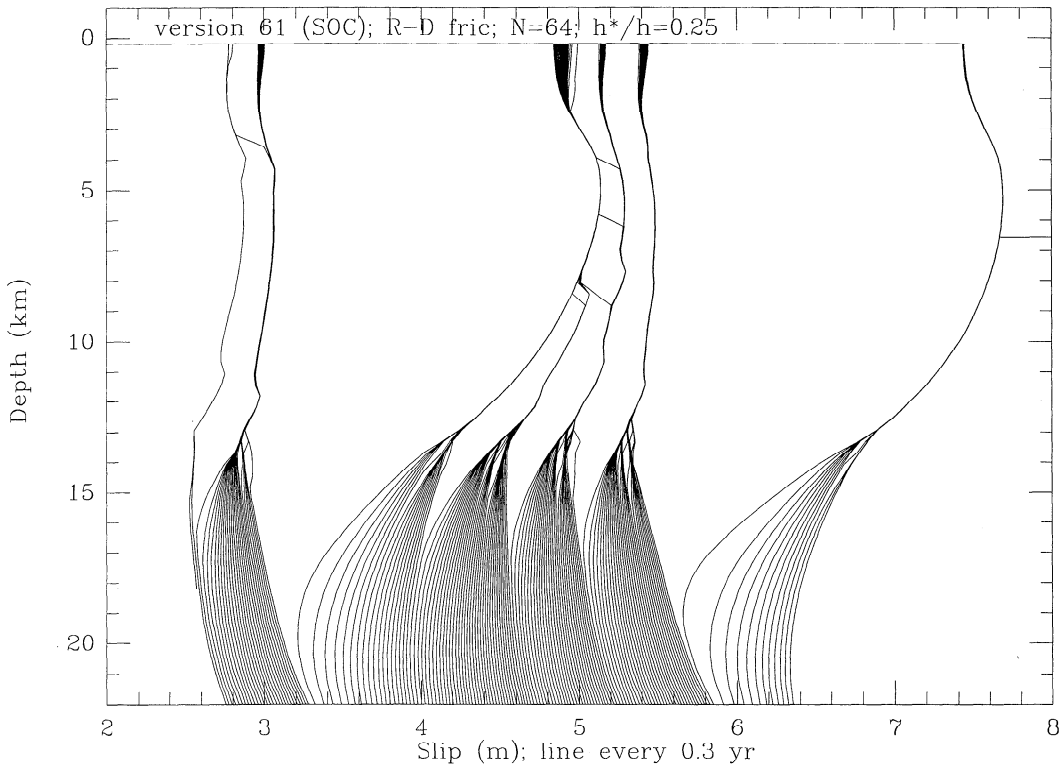

Figure 11. Slip versus depth at 0.3-year interval in dynamic simulation of an inherently discrete case $h = 4h^*$ with the slip version of friction. The creep process is disabled and p is hydrostatic. The results show a range of event sizes including small events.

The simulations of the present work with rate- and state-dependent friction and inertial elastodynamics show nucleation phases, slip instabilities, and dynamic rupture effects. However, event populations simulated on our smooth continuum faults do not have broad frequency-size statistics. This result supports our previous conclusions on the relation between strong fault heterogeneities and spatio-temporal complexity of slip, and it provides additional rationale for the inherently discrete models of *Ben-Zion and Rice* [1993, 1995a] and *Ben-Zion* [1996] as approximate representations of such heterogeneity.

An examination of the results above and results of other similar simulations suggest the following additional features: Rupture is more hesitant and wave phenomena are less pronounced in calculations with the slowness/ageing friction than in simulations with the slip friction. This behavior is compatible with tendencies to develop narrow slip pulses in the former case and crack-like ruptures in the latter [*Perrin et al.*, 1995], although we caution that the rupture events in all cases studied here tend to be crack-like. The logarithmic law effectively saturates the velocity-weakening at high V; it is not yet known whether modifications of that law with enhanced velocity-weakening at high V, which should promote the self-healing rupture mode, would also lead to more complex slip histories in the modeling configuration of Figure 1. Events calculated with the slowness/ageing friction typically start after corresponding events with the slip friction. Final slip values of events in fully dynamic calculations are larger then those of events in corresponding quasi-dynamic calculations. In fully dynamic simulations, final slip values of events in models with the ageing/slowness friction are smaller than those of corresponding events governed by the slip friction (in quasi-dynamic simulations the opposite is generally true). This feature is related to the relative magnitude of the dynamic overshoot in calculations with the different versions of the friction law.

Conclusions

The set of crustal fault models that we have discussed here, with depth-variable rate- and state-dependent friction laws, is similar to the set of rate and state models discussed by *Rice* [1993] and *Ben-Zion and Rice* [1995a]. However, in the present work we do the calculations in the framework of fully inertial elastodynamics with rigorous account of wave-mediated stress transfers, whereas those earlier studies employed a simplified quasi-dynamic procedure. In the quasi-dynamic works, stress transfers ϕ due to slip are calculated by static elasticity, but the exact radiation damping term of (1) is retained, so that solutions continue to exist during instabilities. The major qualitative difference in results is that the fully elastodynamic calculations give richer slip histories during instabilities, with dynamic rupture and wave effects (see, for example, Figure 3b) which are excluded in the quasi-dynamic formulation. However, most other qualitative features of the dynamic response calculated here, particularly whether or not complex slip sequences develop and the relation between slip complexities and strong local heterogeneities, are similar to the earlier results based on the quasi-dynamic analyses.

Our results show that complex slip histories and a broad range of (possibly power law distributed) event sizes are not a

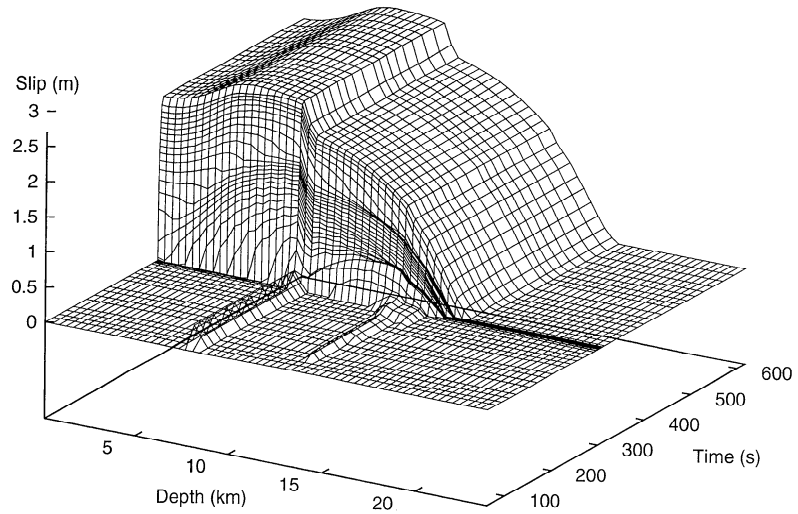

Figure 12. A model earthquake in the simulation leading to Figure 11. The event is preceded by two nucleation phases.

universal feature of dynamic fault models with uniform or smoothly varying properties, despite suggestions to the contrary [e.g., *Myers et al.*, 1996]. It is premature to make the generalization that event sequences in fault models do not have a strong qualitative dependence on whether or not inertial wave-mediated dynamics is incorporated in the calculations. This is because we do not yet have a full understanding of whether our findings apply to other types of models, such as the *Cochard and Madariaga* [1996] fault segment with strong velocity-weakening, or the *Langer et al.* [1996] and *Myers et al.* [1996] crustal plane model with a pair of weakening mechanisms (see the appendix), or even our continuum depth-variable model with some distinctly different class of constitutive laws. Nevertheless, our present results imply that in at least some models the inclusion of full elastodynamics is not decisive to the qualitative nature of the response. The fuller understanding of this issue is important, because the computational demands for full elastodynamics are far more severe than those for the simpler formulations, thus making it impossible at present to study models with highly refined grids to represent both small lab-based h^* and realistic large-scale heterogeneities.

Appendix: Recent Models Showing Dynamic Slip Complexity

Cochard and Madariaga [1996] have analyzed seismic events in a 2-D model with a single large-scale heterogeneity in the form of unbreakable barriers at the edges of a fault segment. Their constitutive properties are homogeneous on the segment, and h^* is well defined and seems to be sufficiently larger than h. Strictly, their model still belongs to the inherently discrete class, because their simulation procedure incorporates an abrupt strength drop at the initiation of failure. However, they recognize explicitly that the small event population thus introduced is an artifact of their numerical procedure. They further suggest, in agreement with *Rice and Ben-Zion* [1996], that those small events would be replaced by an aseismic portion of slip history in a more exact (but more computationally demanding) numerical treatment without the abrupt strength drop, which they use to get quick initiation of events. In general, *Cochard and Madariaga* [1996] find sequences of large events that break most or all of the segment, but by tuning a velocity-weakening parameter in their constitutive law to values comparable to the radiation damping factor they show that the dynamic effects can produce a broad distribution of event sizes within the segment. Essentially, strong heterogeneities of the stress distribution are locked into the segment from event to event, the process being allowed or aided by a self-healing mode of rupture propagation associated with the employed form of velocity-weakening. *Cochard and Madariaga* [1996, Figure A1] also show that even in the parameter range giving a broad distribution of event sizes, as the abrupt strength drop is diminished from 5×10^{-2} to 5×10^{-4} of full strength drop, the population of small numerical artifact events changes character, from one that merges into the population of large events to one that is clearly distinct from it.

Myers et al. [1996] and *Langer et al.* [1996] have examined a 2-D continuum elastic model of a faulted crustal plane coupled to a steadily moving substrate, motivating that as a continuum generalization of the *Burridge and Knopoff* [1967] model of spring-connected blocks (*Johnson* [1992] formulated a crustal plane model of similar type). Myers et al. argue from their dynamic simulations of nominally uniform fault models of such type that complexity, including a broad distribution of large events and a power law distribution of small events, is a universal feature of dynamic fault models. The contrary inertial dynamic results of *Rice and Ben-Zion* [1996], *Cochard and Madariaga* [1996] and the present work show clearly that such complexity is not universal. However, it remains to be understood whether dynamic complexity might be a typical response of certain versions of fault models with constitutive descriptions that include two distinct weakening mechanisms, of very different characteristics (e.g., different strength drops, the first much smaller than the second, and different characteristic slip distances in the weakening processes), as *Langer et al.* [1996] and *Myers et al.* [1996] adopt. *Rice and Ben-Zion* [1996] indicated a simple ambiguity with the above results, stemming from the fact that the first of the two weakening mechanisms has thus far been implemented with an abrupt initial stress drop, leaving some uncertainty, for the reasons discussed above, as to whether a continuum limit is achieved. Thus it remains to be conclusively demonstrated that

the small event distribution and its power law feature is a valid continuum result for a uniform system and not a manifestation of the inherent discreteness effects that *Rice* [1993], *Ben-Zion and Rice* [1993, 1995a], and *Cochard and Madariaga* [1996] have discussed.

A further issue for clarification is that the parameter choice made by *Langer et al.* [1996] and *Myers et al.* [1996] is such that the (well-defined) nucleation size h^* associated with their second, larger strength drop, weakening mechanism has been made comparable to the seismogenic zone depth (on the order of unity in their dimensionless model). This result is related specifically to the choice of value 3 for the parameter α in their model. While we presume that this choice was made for numerical tractability, it is evident from seismic observations that h^* for events of large strength drop must be much smaller than seismogenic zone dimensions. When h^* is small in this sense, initially crack-like events growing from the nucleation size to larger sizes produce a growing stress concentration with increasing rupture dimension and thus become increasingly hard to stop. This is, presumably, why the smooth continuum fault models with small h^* that we have studied dynamically [*Ben-Zion and Rice*, 1995b; *Rice and Ben-Zion*, 1996] and quasi-dynamically [*Rice*, 1993; *Ben-Zion and Rice*, 1995a] do not give a broad distribution of small events. However, when h^* is chosen comparable to the seismogenic thickness in a model of the crustal plane type, the stress concentration from an initially crack-like rupture nucleated at size h^* does not grow so strongly with size increase, and it saturates in magnitude as the crack dimension becomes large. Thus the effect that the large h^* choice has on the complexity of results also remains to be resolved in the crustal plane modeling.

The above problems being stated, it is an appealing conjecture that the combination of two weakening mechanisms with very different characteristics (small strength drop at small slips, perhaps due to unstable Dieterich-type friction, and large strength drop at much larger slips due to subsequent rapid weakening) could contribute to complexity. Such a process can lead to complexity if the large events organize into ruptures that break only part of a uniform model, as reported by *Langer et al.* [1996] and *Myers et al.* [1996], or if strong heterogeneities in fault properties promote such organization. Then there are concentrations of stress left at the ends of each stopped large event. These could serve as nucleation sites for instabilities based on the small slip, small strength drop mechanism, which, under conditions yet to be made fully precise, might not be able to propagate into the length range for instability based on the large slip, large strength drop mechanism. We note that the calculations of *Cochard and Madariaga* [1996], which show complex slip on a fault segment for suitably chosen velocity-weakening parameter, were also based on a constitutive description with two strongly different length scales. In that work the simulated complexity disappeared when the two constitutive length scales were made identical (A. Cochard, private communication, 1996).

Acknowledgments. We thank Alain Cochard, Phillipe Geubelle, John Morrissey, and Gutuan Zheng for discussions on the elastodynamic methodology, and John Morrissey also for help with the plotting procedures. The studies were supported by grants to Harvard from the Southern California Earthquake Center (subcontract 621911 from USC, based on NSF support) and the USGS National Earthquake Hazard Reduction Program (grant 1434-94-G-2450), a visiting professor fellowship to Y.B.-Z. from the Earthquake Research Institute of the University of Tokyo, Japan, and a visiting professorship to J.R.R. from the Department of Geophysics, Stanford University. The paper benefited from comments by Greg Beroza, Alain Cochard, and Steve Day. This is SCEC contribution 365.

References

Andrews, D. J., Dynamic plane-strain shear rupture with a slip-weakening friction law calculated by a boundary integral method, *Bull. Seismol. Soc. Am.*, *75*, 1-21, 1985.

Andrews, D. J., and Y. Ben-Zion, Wrinkle-like slip pulse on a fault between different materials, *J. Geophys. Res.*, *102*, 553-571, 1997.

Beeler, N., T. E. Tullis, and J. D. Weeks, The roles of time and displacement in the evolution effect in rock friction, *Geophys. Res. Lett.*, *21*, 1987-1990, 1994.

Ben-Zion, Y., Stress, slip, and earthquakes in models of complex single-fault systems incorporating brittle and creep deformations, *J. Geophys. Res.*, *101*, 5677-5706, 1996.

Ben-Zion, Y., and J. Morrissey, A simple re-derivation of logarithmic disordering of dynamic planar crack due to small random heterogeneities, *J. Mech. Phys. Solids*, *43*, 1363-1368, 1995.

Ben-Zion, Y., and J. R. Rice, Earthquake failure sequences along a cellular fault zone in a three-dimensional elastic solid containing asperity and nonasperity regions, *J. Geophys. Res.*, *98*, 14,109-14,131, 1993.

Ben-Zion, Y., and J. R. Rice, Slip patterns and earthquake populations along different classes of faults in elastic solids, *J. Geophys. Res.*, *100*, 12,959-12,983, 1995a.

Ben-Zion, Y., and J. R. Rice, Slip along a crustal-scale fault governed by rate- and state-dependent friction and inertial elastodynamics (abstract), *Eos Trans. AGU*, *76* (46), Fall Meet. Suppl., F405, 1995b.

Blanpied, M. L., D. A. Lockner, and J. D. Byerlee, Fault stability inferred from granite sliding experiments at hydrothermal conditions, *Geophys. Res. Lett.*, *18*, 609-612, 1991.

Burridge, R., and L. Knopoff, Model and theoretical seismicity, *Bull. Seismol. Soc. Am.*, *57*, 341-371, 1967.

Cochard, A., and R. Madariaga, Dynamic faulting under rate-dependent friction, *Pure Appl. Geophys.*, *142*, 419-445, 1994.

Cochard, A., and R. Madariaga, Complexity of seismicity due to highly rate-dependent friction, *J. Geophys. Res.*, *101*, 25,321-25,336, 1996.

Cochard, A., and J. R. Rice, A spectral method for numerical elastodynamic fracture analysis without spatial replication of the rupture event, *J. Mech. Phys. Solids*, in press, 1997.

Dieterich, J. H., Modeling of rock friction, 1, Experimental results and constitutive equations, *J. Geophys. Res.*, *84*, 2161-2168, 1979.

Dieterich, J. H., Constitutive properties of faults with simulated gouge, in *Mechanical Behavior of Crustal Rocks: The Handin Volume*, *Geophys. Monogr. Ser.*, vol. *24*, *edited by N. L. Carter et al.*, pp. 103-120, AGU, Washington, D. C., 1981.

Dieterich, J. H., Earthquake nucleation on faults with rate- and state-dependent strength, *Tectonophysics*, *211*, 115-134, 1992.

Geubelle, P., and J. R. Rice, A spectral method foe three-dimensional elastodynamic fracture problems, *J. Mech. Phys. Solids*, *43*, 1791-1824, 1995.

Harris, R. A., and S. M. Day, Effects of a low-velocity zone on a dynamic rupture, *Bull. Seismol. Soc. Am.*, in press, 1997.

Heaton, T. H., Evidence for and implications of self-healing pulses of slip in earthquake rupture, *Phys. Earth Planet. Inter.*, *64*, 1-20, 1990.

Johnson, E., The influence of the lithospheric thickness on bilateral slip, *Geophys. J. Int.*, *108*, 151-160, 1992.

Knopoff, L., The organization of seismicity on fault networks, *Proc. Natl. Acad. Sci. U. S. A.*, *93*, 3830-3837, 1996.

Lachenbruch, A. H., Frictional heating, fluid pressure, and the resistance to fault motion, *J. Geophys. Res.*, *85*, 6097-6112, 1980.

Langer, J. S., J. M. Carlson, C. R. Myers, and B. E. Shaw, Slip complexity in dynamic models of earthquake faults, *Proc. Natl. Acad. Sci. U. S. A.*, *93*, 3825-3829, 1996.

Lockner, D. A., and J. D. Byerlee, An earthquake instability model based on faults containing high fluid-pressure compartments, *Pure Appl. Geophys.*, *145*, 717-745, 1995.

Madariaga, R., and A. Cochard, Dynamic friction and the origin of the complexity of earthquake sources, *Proc. Natl. Acad. Sci. U. S. A.*, *93*, 3819-3824, 1996.

Melosh, H. J., Acoustic fluidization: A new geological process?, *J. Geophys. Res.*, *84*, 7513-7520, 1979.

Miller, S. A., Fluid-mediated influence of adjacent thrusting on the seismic cycle at Parkfield, *Nature, 382*, 799-802, 1996.

Miller, S. A., A. Nur, and D. L. Olgaard, Earthquakes as a coupled shear stress-high pore pressure dynamical system, *Geophys. Res. Lett., 23*, 197-200, 1996.

Morrissey, J., and J. R. Rice, 3D elastodynamics of cracking through heterogeneous solids: crack front waves and growth of fluctuations (abstract), *Eos Trans. AGU, 77*(44), Fall Meet. Suppl., F485, 1996.

Myers, C. R., B. E. Shaw, and J. S. Langer, Slip complexity in a crustal-plane model of an earthquake fault, *Phys. Rev. Lett., 77*, 972-975, 1996.

Ohnaka, M., Nonuniformity of the constitutive law parameters for shear rupture and quasistatic nucleation to dynamic rupture: A physical model of earthquake generation processes, *Proc. Natl. Acad. Sci. U. S. A., 93*, 3795-3802, 1996.

Okubo, P. G., Dynamic rupture modeling with laboratory-derived constitutive relations, *J. Geophys. Res., 94*, 12,321-12,335, 1989.

Perrin, G., and J. R. Rice, Disordering of a dynamic planar crack front in a model elastic medium of randomly variable toughness, *J. Mech. Phys. Solids, 42*, 1047-1064, 1994.

Perrin, G., J. R. Rice, and G. Zheng, Self-healing slip pulse on a frictional surface, *J. Mech. Phys. Solids, 43*, 1461-1495, 1995.

Rice, J. R., The mechanics of earthquake rupture, in *Physics of the Earth's Interior*, edited by. A. M. Dziewonski and E. Boschi, pp. 555-649, Ital. Phys. Soc./North-Holland, New York, 1980.

Rice, J. R., Spatio-temporal complexity of slip on a fault, *J. Geophys. Res., 98*, 9885-9907, 1993.

Rice, J. R., Earthquakes at low driving stress in a high strength, low toughness fault zone: Shear-heating example (abstract), *Eos Trans. AGU, 75* (44), Fall Meeting Suppl., 426, 1994a.

Rice, J. R., Comparison of slip complexity produced by two rate- and state-dependent friction laws (abstract), *Eos Trans. AGU, 75* (44), Fall Meet. Suppl., 441, 1994b.

Rice, J. R., and Y. Ben-Zion, Slip complexity in earthquake fault models, *Proc. Natl. Acad. Sci. U. S. A., 93*, 3811-3818, 1996.

Rice, J. R., Y. Ben-Zion, and K. S. Kim, Three-dimensional perturbation solution for a dynamic planar crack moving unsteadily in a model elastic solid, *J. Mech. Phys. Solids, 42*, 813-843, 1994.

Ruina, A., Slip instability and state variable friction laws, *J. Geophys. Res., 88*, 10,359-10,370, 1983.

Sharon, E., S. P. Gross, and J. Fineberg, Local crack branching as a mechanism for instability in dynamic fracture, *Phys. Rev. Lett., 74*, 5096-5099, 1995.

Shibazaki, B., and M. Matsu'ura, Spontaneous processes for nucleation, dynamic propagation, and stop of earthquake rupture, *Geophys. Res. Lett., 19*, 1189-1192, 1992.

Sleep, N. H., and M. L. Blanpied, Creep, compaction and the weak rheology of major faults, *Nature, 359*, 687-692, 1992.

Tse, S. T., and J. R. Rice, Crustal earthquake instability in relation to the depth variation of frictional slip properties, *J. Geophys. Res., 91*, 9452-9472, 1986.

Tsutsumi, A., and T. Shimamoto, High-velocity frictional properties in gabbro, *Geophys. Res. Lett., 24*, 699-702, 1997.

Weertman, J., Unstable slippage across a fault that separates elastic media of different elastic constants, *J. Geophys. Res., 85*, 1455-1461, 1980.

Yoffe, E. H., The moving Griffith crack, *Philos. Mag., 42*, 739-750, 1951.

Zheng, G., Y. Ben-Zion, J. R. Rice, and J. Morrissey, A new method for calculating elastodynamic response over long stressing histories containing rapid rupture episodes (abstract), *Eos Trans. AGU, 76*(46), Fall Meet. Suppl., F405, 1995.

Y. Ben-Zion, Department of Earth Sciences, University of Southern California, Los Angeles, CA 90089-0740. (e-mail: benzion@jade.usc.edu)

J. R. Rice, Department of Earth and Planetary Sciences, Harvard University, Cambridge, MA 02138. (e-mail: rice@esag.harvard.edu)

(Received October 22, 1996; revised April 23, 1997;
accepted April 30, 1997.)